# Thin Film $WSe_2$ for Use as a Photovoltaic Absorber Material

Qinglei Ma, Hrachya Kyureghian, Joel D. Banninga and N. J. Ianno

Department of Electrical Engineering, University of Nebraska, 209N WSEC Lincoln, NE 68588-0511

## ABSTRACT

An excellent candidate for an earth abundant absorber material is $WSe_2$ which can be directly grown as a p-type semiconductor with a band gap near 1.4 eV. In this work we present the structural, optical, and electrical properties of thin film $WSe_2$ grown via the selenization of sputter deposited tungsten films. We will show that highly textured films with an optical band gap in range of 1.4 eV, and absorption coefficients greater than $10^5$/cm across the visible spectrum can be easily achieved. In addition we will present Hall Effect and carrier density measurements as well, where will show densities in the $10^{17}cm^{-3}$ range and p-type Hall mobilities greater than 10 $cm^2$/V-s range can be obtained. We employ these results to numerically simulate solar cells based on this material, where we will show efficiencies greater than 20% are possible.

## INTRODUCTION

Tungsten selenide was first pointed out as a possible photovoltaic absorber in an early compilation of band gaps for some materials. [1] Some of the early studies record a band gap of 1.35 eV, very close to the optimal value of 1.36 eV for a single-junction solar cell. Recently the single crystal band gaps have been determined to be 1.545 eV and 1.486 eV for the direct and indirect single crystal band gaps respectively. [2] In addition it has only one stable crystalline structure at room temperature. [2] Also W and Se do not form a stable compound of any stoichiometry other than $WSe_2$. It should be mentioned that amorphous $WSe_3$ decomposes to $WSe_2$ at 220 $^oC$. [3] Bulk crystals have been doped p and n-type, leading to the possibility of homojunction devices, and some heterojunction single crystal photovoltaic devices with efficiencies in excess of 8 % have been fabricated. [4]

Several methods were adopted to prepare $WSe_2$ thin films in previous research. [5-10] In this paper, $WSe_2$ thin films were prepared by selenization of tungsten films under 1 atmosphere selenium pressure in a closed tube in a single-zone furnace. All $WSe_2$ thin films synthesized under different temperatures are highly oriented with the c axis predominantly perpendicular to the substrate. The mobility of $WSe_2$ thin films varied with processing temperature and rises to 30 $cm^2$/V-sec at 875 $^oC$.

In view of these favorable attributes we have employed PC1D to simulate the performance of homojunction photovoltaic devices based on $WSe_2$. The input parameters for the simulation are obtained through a combination of existing literature and direct measurements performed on thin films grown as described above. We will show that homojunctions devices have the potential to exceed 20 % efficiency.

## EXPERIMENT

### Film growth

Tungsten films of about 100 nm thickness were DC-sputtered from a 99.5% pure tungsten target onto 15 mm x15 mm quartz substrates at room temperature. The substrates were thoroughly cleaned prior to insertion into the vacuum chamber with a base pressure of 1.33 $x10^{-4}$ Pa. Before the tungsten films were deposited onto the substrates the target itself was pre-sputtered for 5-10 minutes to clean away oxides on its surface. The operating argon pressure was kept constant at 0.133 Pa during sputtering. The sputtering power was set to 40 Watt yielding a deposition rate of about 3 nm/s. In order to obtain a uniform film, the substrate was rotated at 20 revolutions per minute.

A tungsten film and selenium powder (99.999%) were sealed into a quartz tube evacuated to $1.33x10^{-5}$ Pa. The amount of selenium was controlled to yield 1 atmosphere of Se pressure at the process temperature. The sealed tubes were placed into a room temperature furnace and ramped to the process temperature at a rate of 4 C/min, soaked for 20 hours and ramped down to room temperature at the same rate. Processing temperatures from 825 ºC to 900 ºC with a step of 25 ºC were investigated. The results presented here clearly show that a single zone, single step process can produce high quality $WSe_2$ films.

### Raman spectroscopy

In order to determine lattice dynamics of $WSe_2$ thin films, Raman spectra of both a $WSe_2$ commercially purchased single crystal and our films are investigated by Raman spectroscopy employing a 633 nm excitation laser and 2400 $mm^{-1}$ grating. Figure 1 shows the Raman spectra of the single crystal and the films processed at 875 ºC and 900 ºC. Both the $E_{2g}{}^1$ and $A_{1g}$ modes, are present in the crystal and the films. [11]

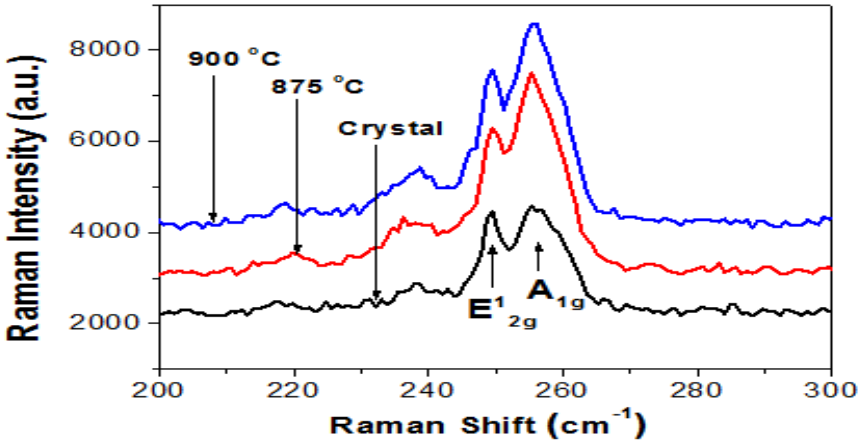


**Figure 1**. Raman Spectra of $WSe_2$ crystal and thin films.

### X-ray diffractometry

The x-ray diffraction patterns (CuKα anode) seen in Figure 2 indicate that the films exhibited the 2H-$WSe_2$ hexagonal structure. The three primary peaks in the spectrum correspond to the (002), (006), (008), showing that the c axis is perpendicular to the substrate. It should be noted

that the double peak at the (002) plane is a result of the fact that the x-ray source is not monochromatic so a peak from the CuKα2 emission line is observed. The average grain size as determined by the Debye Scherrer formula is approximately 80nm for both films.

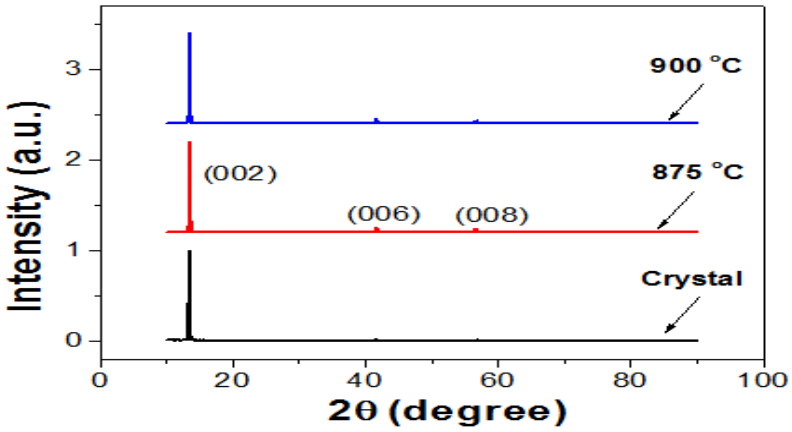


**Figure 2.** X-ray diffraction patterns of the $WSe_2$ thin films.

## Optical characterization

In this work, variable angle spectroscopic ellipsometry characterization of a $WSe_2$ single crystal sample and $WSe_2$ thin films at three angles (55°, 65°, 75°) across the 350 nm-1700 nm wavelength was performed. The thickness of the tungsten selenide film is determined by profilometry and is about four times thicker than the original tungsten film. The measured film thickness was employed in the ellipsometry analysis where the final film thicklness was within 10% of the measured value. The MSEs are between 12 and 17 for different $WSe_2$ thin films. The dispersion of the refractive index n and extinction coefficient k of $WSe_2$ thin films, as well as $WSe_2$ crystal, are shown in Fig. 3. We can observe that all films share the similar n and k curve shapes with $WSe_2$ crystal. The extinction coefficient k is in good agreement with previous results.[7]

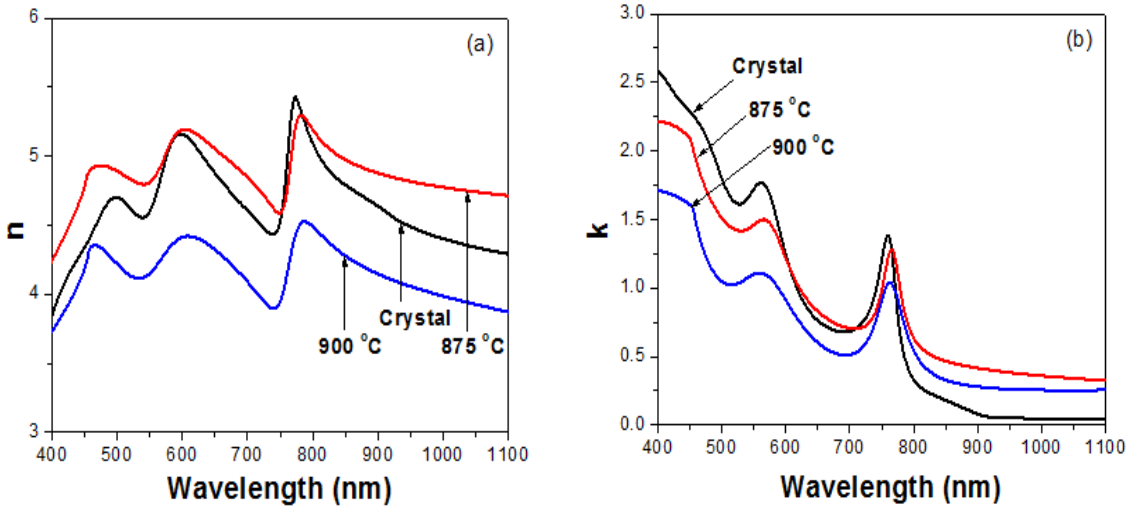


**Figure 3**. The dispersion of the refractive index n (a) and extinction coefficient k (b) of $WSe_2$ thin films, and single crystal.

Transmission data was also acquired for the films, and this data was used to generate the abosprtion coefficient. The absorption coefficient was also generated from the extinction coefficient obtained through ellipsometry. Tauc plots to determine the dierct and indirect band gaps were generated from both sets of abosrption coefficients as seen in Figure 4.

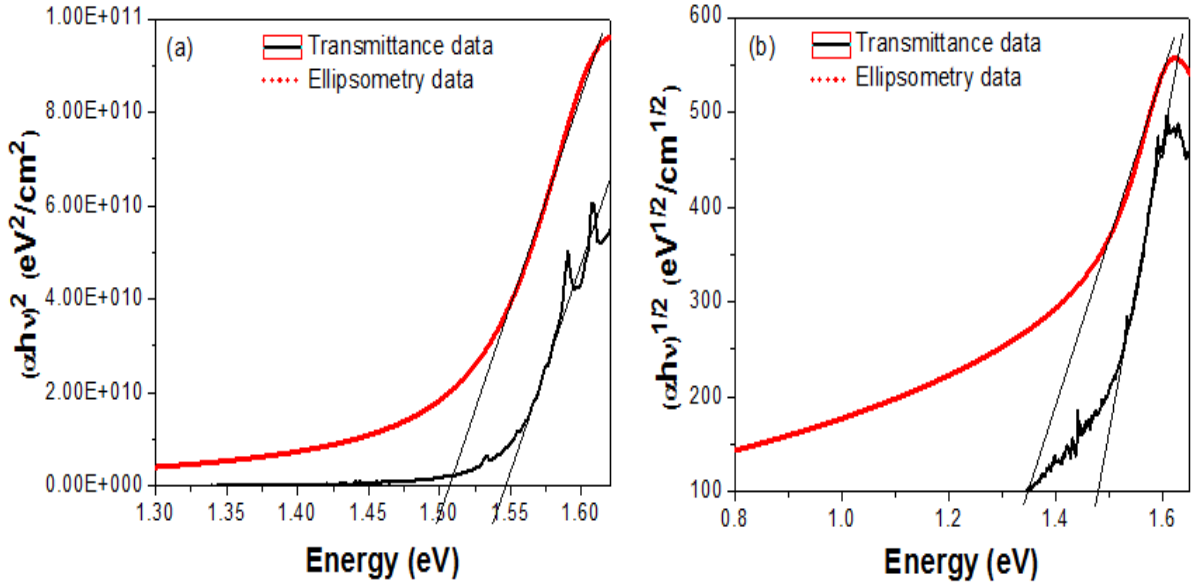


**Figure 4.** Tauc plots of a $WSe_2$ thin film from both transmittance and ellipsometry data. (a) Direct band gap, (b) Indirect band gap. The $WSe_2$ thin film is made at 875 $^oC$.

As can be seen the figure the band gaps differ by about 5% with ellipsometry yielding a smaller gap.

## Electronic characterization

Electrical transport properties, including the mobility, resistivity and carrier concentration, are investigated by performing Hall Effect and four point probe measurements. All tests are performed at room temperature. A magnetic field of 1.3 T is employed while silver paint is used as the metal contact. All films are as-grown p-type where those grown at 875 $^oC$ and 900 $^oC$ exhibit Hall mobilities of 30 $cm^2V^{-1}sec^{-1}$ and a carrier concentrations of around $10^{17}$ $cm^{-3}$.

## Photovoltaic device simulation

In order to obtain an idea of the potential device performance PC1D was employed to simulate an ideal homojunction device consisting of a 1 micron thick p-type absorber layer, $p=10^{17}$ $cm^{-3}$, $\mu = 30$ $cm^2V^{-1}sec^{-1}$ (data obtained from the as-grown films), with the band gap and absorption coefficient also obtained from the as-grown films. A 50 nm $WSe_2$ n-type layer, $n= 10^{19}$ $cm^{-3}$, $\mu = 1$ $cm^2V^{-1}sec^{-1}$ was employed as the window. The illumination was set at 1.5AMG. All other needed parameters were taken from the literature, determined from as-grown films or calculated from the literature data. [10-15] Figure 5 shows the results of the simulation where the efficiency is plotted as a function of the carrier lifetime. For lifetimes in the ns range the

efficiency is between 10 and 15%. A well designed heterojunction may yield even higher efficiency.

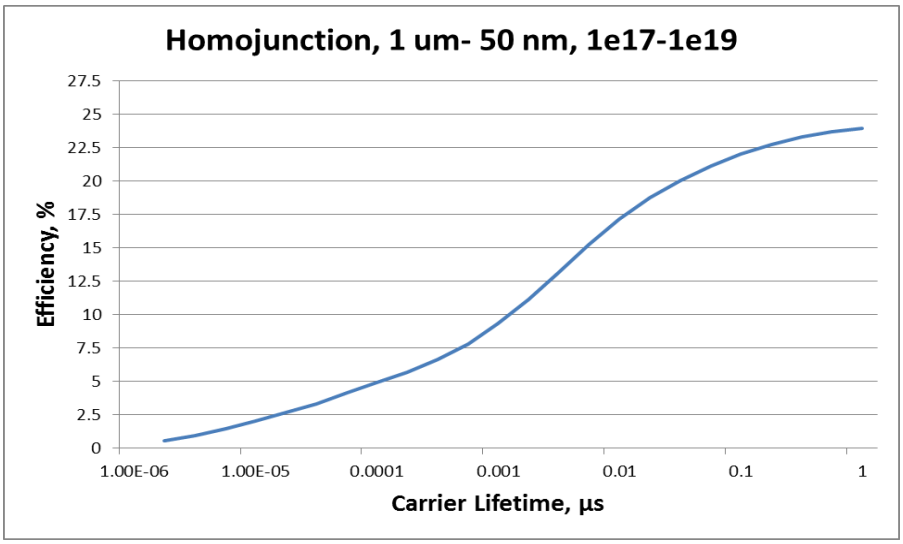


**Figure 5.** PC1D simulation of WSe2 homojunction photovoltaic device under 1.5AMG illumination.

## CONCLUSIONS

Thin films of $WSe_2$ have been grown in a single step by single zone selenization of sputter deposited tungsten films. When grown under 1 atmosphere of selenium pressure at 875 or 900 $^oC$ p-type films where $p=10^{17}$ $cm^{-3}$, and $\mu = 30$ $cm^2V^{-1}sec^{-1}$ are reproducibly obtained. In addition the absorption coefficient is above $10^5$ $cm^{-1}$ over the 400-900nm spectral range and the resultant indirect band gap as determined by spectroscopic ellipsometry is 1.36 eV and the direct band gap is 1.51 eV. Simulation of a homojunction device based on the parameters of the as-grown films and literature values yields an efficiency of 10% for a 1 ns bulk carrier lifetime increasing up to values greater than 20% for long lifetimes.


## ACKNOWLEDGMENTS

This work is supported by NSF grant 1004094 and the Nebraska Center for Sciences Research.


## REFERENCES


1. W.H. Strehlow and E.L. Cook , *Journal of Physical and Chemical Reference Data* **2,** 163 (1973).
2. Jain, S-P Ong, G. Hautier, W. Chen, W.D. Richards, S. Dacek, S. Cholia, D. Gunter, D. Skinner, G. Ceder, and K.A. Perssonn, *APL Materials* **1**, 011002 (2013).

3. E. LASSNER and W-D.SCHUBERT, *Tungsten: Properties, Chemistry, Technology of the Element, Alloys, and Chemical Compounds* Kluwer Academic / Plenum Publishers, New York in 1999.
4. M. Ch. Lux-Steiner, M. Võgt, P. Dolatzoglou, A. JãgerWaldau and E. Bucher, Technical Digest 3rd Int. Photovoltaic Science and Engineering Conference, Tokyo, Japan, 687 (1987).
5. Jager-Waldau and E. Bucher, *Thin Solid Films* **200,** 157 (1991).
6. J. Pouzet, J. C. Bernede, A. Khellil, H. Essaidi and S. Benhida, *Thin Solid Films* **208,** 259 (1992).
7. G. Salitra, G. Hodes, E. Klein, and R. Tenne, *Thin Solid Films* **245** 180, (1994).
8. J. Jebaraj Devadasan, C. Sanjeeviraja and M. Jayachandran *Materials Chemistry and Physics* **77,** 397 (2002).
9. P.P. Hankare, A.H. Manikshete, D.J. Sathe, P.A. Chate and K.C. Rathod *Materials Chemistry and Physics* **113**, 183-186 (2009).
10. S.N. Grigoriev, V.Yu. Fominski, A.G. Gnedovetsand R.I. Romanov, *Applied Surface Science* **258** 7000 (2012).
11. P. Tonndorf, R. Schmidt, P. Böttger, X. Zhang, J. Börner, A. Liebig, M. Albrecht, C. Kloc, O. Gordan, D. R. T. Zahn, S. Michaelis de Vasconcellos and Rudolf Bratschitsch, *Optics Express* **21** 4908-4916 (2013).
12. O. Lang, Y. Tomm, R. Schalf, C. Pettenkofer and W. Jaegermann, *Journal of Applied Physics* **75**, 7814 (1994).
13. B. Davey, and B.L. Evans, *Physica Status Solidi A* **13** , 483 (1972).
14. G.K. Solanki, D.N. Gujarathi, M.P. Deshoande, D. Lakshminarayana and M.K. Agarwal, Crystal Research and Technology **43** (2), 179–185 (2008).
15. K.K. Patel, K. D Patel, M. Patel, C.A. Patel, V.M. Pathak and R. Srivastava, *AIP Conference Proceedings* **1393**, 251 (2011).